Bioorganic Chemistry 92 (2019) 103226

Contents lists available at ScienceDirect

Bioorganic Chemistry

journal homepage: www.elsevier.com/locate/bioorg

Chemical constituents from Alismatis Rhizoma and their anti-inflammatory activities *in vitro* and *in vivo*

Shan-shan Liu[a,b,1], Wen-long Sheng[c,1], Yun Li[a], Shan-shan Zhang[c], Jing-jing Zhu[a], Hui-min Gao[a], Li-hua Yan[a,*], Zhi-min Wang[a,*], Lu Gao[d], Mei Zhang[b]

[a] National Engineering Laboratory for Quality Control Technology of Chinese Herbal Medicines, Institute of Chinese Materia Medica, China Academy of Chinese Medical Sciences, Beijing 100700, China
[b] Beijing Key Laboratory of Organic Materials Testing Technology and Quality Evaluation, Beijing Center for Physical and Chemical Analysis, Beijing 100089, China
[c] Biology Institute, Qilu University of Technology (Shandong Academy of Sciences), Jinan 250103, China
[d] Xiuzheng Pharmaceutical Group Co., Ltd, Tonghua 134000, China

ARTICLE INFO

Keywords:
Alismatis Rhizoma
2, 4, 6-cycloheptatrien ketone
Diphenylpropanoid ether
Triterpenoid
Anti-inflammatory

ABSTRACT

Six new compounds, including a new compound with an unusual 2, 4, 6-cycloheptatrien ketone skeleton (**1**), two new diphenylpropanoid ethers (**2**, **3**), a new protostane-type triterpenoid (**4**), two new norsesquiterpene (**5a**, **5b**), and two new natural products (**6**, **7**), together with eleven known compounds (**8**–**18**) were isolated from the aqueous extract of Alismatis Rhizoma (AR). Their structures were elucidated by a combination of 1D and 2D NMR (^{1}H and ^{13}C NMR, COSY, HSQC, HMBC, and NOESY), HRESIMS spectroscopic data, experimental and calculated electronic circular dichroism (ECD) spectra. Some of the compounds were evaluated for their inhibitory effects on nitric oxide (NO) production in LPS-induced RAW 264.7 cells. Two protostane-type triterpenoids, compounds **4** and **17**, exhibited potent inhibitory activities with the IC_{50} values of 39.3 and 63.9 μM compared with indomethacin. In the meanwhile, their anti-inflammatory effects were also confirmed by acute inflammation model induced by $CuSO_4$ in zebrafish.

1. Introduction

The genus *Alisma* comprises 11 species and widely distributes in the temperate and subtropical regions all over the world [1], of which *Alisma orientale* (Sam.) Juzep is mainly distributed in China, Japan, North America, and Europe [2]. *Alisma orientale* is a herbaceous plant growing in bogs, which is widely cultured in Sichuan and Fujian provinces of China for two hundreds of years [3]. The dried rhizome of it (Alismatis Rhizoma, AR) is an important component of many famous Chinese medicine prescriptions, such as Zexie Decoction, Wuling Powder, and Liuweidihuang Formula, to treat dysuria, edema, obesity, diabetes, hyperlipidemia, and hypertension [4]. AR has been recorded in the Chinese Pharmacopoeia since 1963 and is also widely used in Japan [4]. In addition, the stems of the plants can be eatable as vegetables in Fujian and Jiangxi Provinces of China. Previous phytochemical investigations on AR have disclosed the presence of protostane-type triterpenoids, sesquiterpenes, including those with guaiane, eudesmane and germacrane skeletons, as well as saccharides [5,6], phenylpropanoids [7], flavones, and nitrogen compounds [4,8]. Among them, protostane-type triterpenoids were considered to be the primary active ingredients. The modern pharmacological studies showed that the water, ethanol or methanol extracts of AR, along with the protostane-type triterpenoids, such as alisol B 23-acetate, alisol B, alisol A, and alisol A 24-acetate, exhibited diuretic [9–11], anti-hyperlipidemia [12–15], antidiabetic [16], anti-oxidative [17], anti-tumor [18–21], anti-allergic [22,23], anti-inflammatory [24,25], and anti-complementary [26] activities.

Water decoction was mostly used in traditional Chinese clinical treatment. However, most of the bioactive constituents, triterpenoids, and sesquiterpenes, were isolated from ethanol or methanol extracts of AR. These compounds were lipophilic and seldom detected in water decoction. Previous studies indicated that the aqueous extract of AR possesses hypoglycemic [16], cytoprotective, and antioxidative activities [27]. For the chemical compositions, only polysaccharides [6,28–30], few monosaccharides, and oligosaccharides [5] were revealed from it. According to the results of our chemical investigation, the yield of aqueous extract of AR was almost 20% (w/w), of which the fractions of polysaccharides were about 6% accounting for the dried

* Corresponding authors.
E-mail addresses: lhyan@icmm.ac.cn (L.-h. Yan), zmwang@icmm.ac.cn (Z.-m. Wang).
[1] These authors contributed equally to this work.

https://doi.org/10.1016/j.bioorg.2019.103226
Received 29 January 2019; Received in revised form 30 June 2019; Accepted 27 August 2019
Available online 28 August 2019

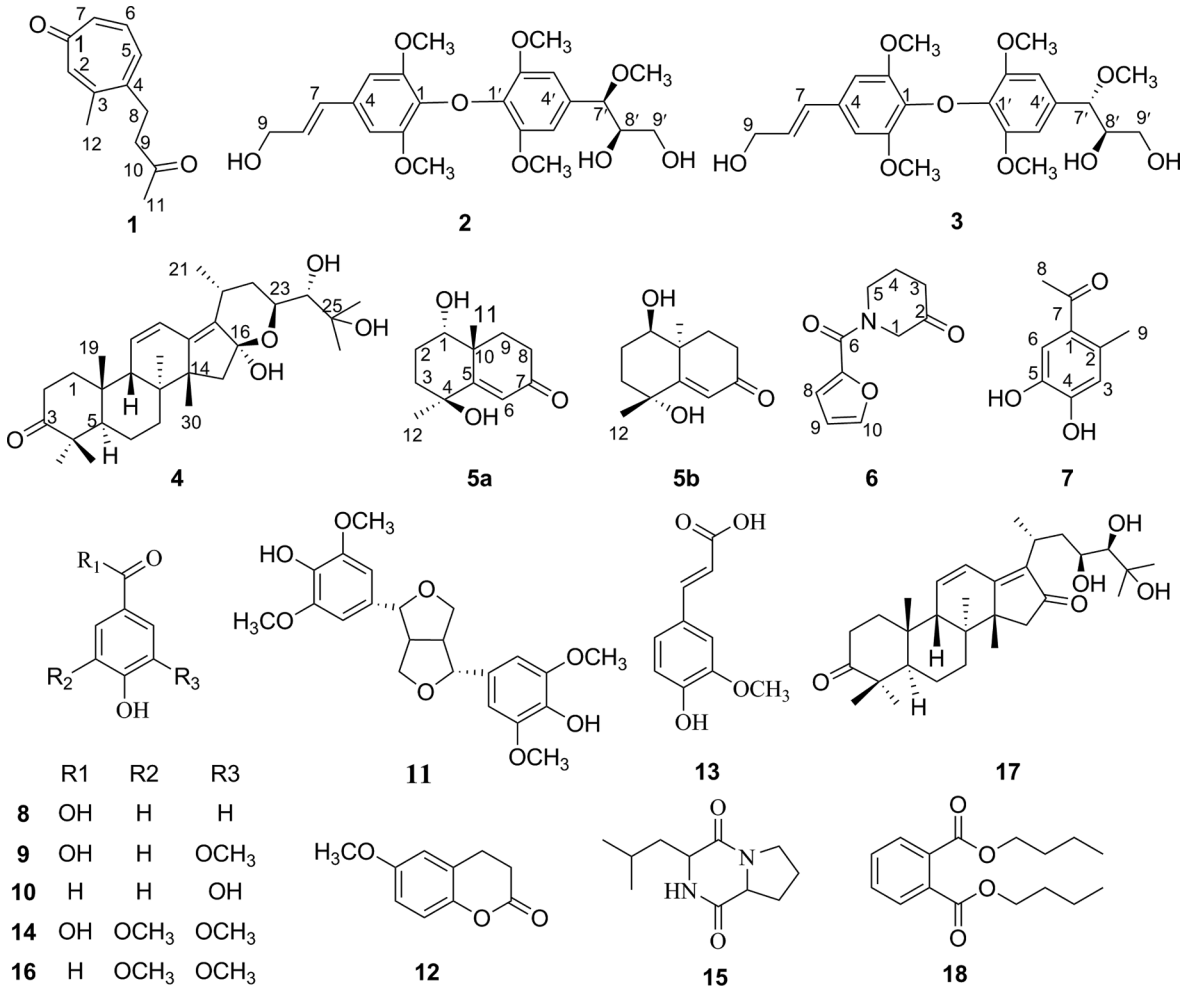

Fig. 1. Structures of compounds **1–18**.

AR, as well triterpenoids and sesquiterpenes were less than 1.5%. The most of the compounds in the remaining aqueous extract were still unknown. Then, the further investigation on water-soluble constituents would be helpful to reveal the effective substances of AR in pharmaceutical applications.

As we all know, inflammation is a normal biological response to injury and infection. However, it would develop to diseases pathogenesis during chronic or excessive activation of the immune system, which was related to a series of diseases. Nitric oxide (NO), produced from L-arginine by nitric oxide synthase, is a well-known cellular signaling molecule, and the overproduction of NO can cause inflammation [31]. The level of NO was used as an inflammatory biomarker. As to the *in vivo* models, zebrafish (*Danio rerio*) has become a popular one in the fields of drug development and toxicology [32,33]. It has well-developed innate and acquired immune systems, which are highly consistent with those of the mammal [34]. Therefore, it was also widely used for screening anti-inflammatory agents [35–37].

In the present study, nineteen compounds with diverse structures were isolated from the aqueous extract of AR, including six new chemical constituents, two new natural products, and eleven known ones (Fig. 1). The inhibitory effects of the isolated compounds on LPS-induced NO production in RAW 264.7 cells were evaluated and their anti-inflammatory effects were also evidenced by acute inflammation model induced by $CuSO_4$ in zebrafish.

2. Materials and methods

2.1. General experimental procedures

Optical rotations were measured on a PE Model 343 digital polarimeter (Perkin-Elmer, Waltham, U.S.A). UV spectra were determined by a JASCO V-650 spectrophotometer (JASCO, Tokyo, Japan). NMR spectra were recorded on a Bruker Avance 600 spectrometer (Bruker Biospin, Fallanden, Switzerland), using TMS as internal standard. HRESIMS data were obtained on a Waters Xevo G2-S QTOF instrument (Waters, Milford, USA). ECD spectra were recorded on a J-815 spectrometer (JASCO, Tokyo, Japan) and Chirascan circular dichroism (Applied Photophysics, Leatherhead, UK). IR spectra on a Nicolet 5700 spectrometer (Thermo Electron Corporation, Madison, WI, USA) using an FT-IR microscope transmission method. Middle pressure liquid chromatography (MPLC) was performed on a Biotage Isolera Prime chromatography system (Biotage, Uppsala, Sweden). High-performance liquid chromatography (HPLC) was applied with a Shimadzu HPLC system, including a pump model LC-20AT and a UV detector model SPD-M20 (Shimadzu Inc., Kyoto, Japan). The preparative HPLC was performed on a QuikSep instrument (H&E Co., Ltd., Beijing, China) with a UV detector. Two HPLC columns (Welch Ultimate XB-C_{18}, 20 × 250 mm, 10 μm and Kromasil 100–5 C_{18}, 250 × 10 mm, 5 μm) were applied in the purification. HPD-500 macroporous absorbent resin (Hebei Bonherb Technology Corp., Cangzhou, China), silica gel (200–300 mesh, Qingdao Marine Chemical Factory, Qingdao, China), reversed-phase C_{18} silica gel (50 μm, YMC Co. Ltd., Kyoto, Japan) and Sephadex LH-20 (GE healthcare, Uppsala, Sweden) were used for

Table 1
^{1}H(600 MHz) and ^{13}C(150 MHz) NMR data for compounds **1** and **5–7** in CD_3OD (*J* in Hz).

No	1		5		6		7	
	δ_H	δ_c	δ_H	δ_c	δ_H	δ_c	δ_H	δ_c
1		187.7	3.43, m	73.0	4.64, s	49.6		127.9
2	7.16, d, 2.8	141.5	α 2.04, m; β 1.71, m	26.0		178.7		132.5
3		149.9	α 1.55, dt, 12.2, 3.7; β 2.07, m	33.6	2.45, t, 8.1	31.5	6.65, s	118.4
4		151.2		71.0	2.13, m	19.1		149.2
5	7.10, d, 9.1	133.3		176.5	3.53, t, 7.1	49.7		142.3
6	7.28, dd, 11.7, 9.1	137.5	6.26, s	123.8		184.4	7.34, s	117.8
7	6.94, dd, 11.7, 2.8	138.0		201.7		152.4		200.6
8	2.88, m	31.0	α 2.25, d, 11.1; β 2.51, d, 10.6	33.2	7.42, d, 3.6	119.6	2.50, s	27.6
9	2.83, m	42.5	α 2.52, d, 10.6; β 1.41, dd, 8.6, 2.2	33.4	6.67, dd, 3.6, 1.6	113.6	2.40, s	20.5
10		207.9		40.9	7.82, d, 1.0	149.1		
11	2.19, s	28.4	1.23, s	22.9				
12	2.42, d, 0.6	24.4	1.31, s	29.4				

column chromatography (CC). TLC analysis was performed on pre-coated silica gel GF_{254} plates (Qingdao Marine Chemical Factory, Qingdao, China).

2.2. Plant material

AR was purchased from Sichuan Golden Land Group Co., Ltd., Chengdu, China. It was identified according to the Chinese Pharmacopoeia (2015 version) by Prof. Li-hua Yan from the Institute of Chinese Materia Medica, China Academy of Chinese Medical Sciences, Beijing, China, where a voucher specimen (No. XZZX20170802) was deposited and the content of alisol B 23-acetate in it was 0.10%, which accorded with the stipulation of Chinese Pharmacopoeia (2015 version).

2.3. Extraction and isolation

Dried AR (100 kg) were powdered and soaked in distilled water for 12 h, then extracted under reflux (800 L × 2 h × 2) and filtered. The aqueous solution was subjected to macroporous absorbent resin column (100 L), and partitioned successively with water (96 L), 20% EtOH (720.8 g), 50% EtOH (747.6 g), 70% EtOH (413.8 g), and 95% EtOH (95.9 g) (96 L × 3). The 50% EtOH-eluted (677.6 g) part was subjected to silica gel CC, eluted with petroleum ether (PE)-acetone (7:1–1:1) and finally washed with MeOH to afford twelve fractions (A–L).

Fraction E (55.8 g) was applied to silica gel CC with CH_2Cl_2-acetone (9:1–1:1) to give ten fractions (E1-E10). Fraction E2 (7.6 g) was fractionated by silica gel CC using PE-acetone (5:1–1:1) to afford eight subfractions (E2.1-E2.8). Further purification of fraction E2.3 (1.05 g) via silica gel CC elution with petroleum CH_2Cl_2-MeOH (65:1) and preparative HPLC elution with CH_3CN-H_2O (10:90–12:88) yielded compound **7** (4 mg). Separation of fraction E2.4 (1.16 g) by silica gel CC with CH_2Cl_2-MeOH (75:1) afforded five subfractions (E2.4.1-E2.4.5). Subfraction E2.4.2 (508 mg) was separated by preparative HPLC elution with CH_3CN-H_2O acidified with 0.1% formic acid (8:92–12:88) to yield compound **9** (22 mg). Compounds **10** (4 mg) and **8** (7.3 mg) were obtained from subfractions E2.4.4 (228 mg) and E2.4.5 (124 mg) by preparative HPLC (CH_3CN-H_2O acidified with 0.1% formic acid, 7:93 and 5:95, respectively). Fraction E2.5 (1.57 g) was fractionated via silica gel CC with CH_2Cl_2-MeOH (100:1) and then purified by preparative HPLC (CH_3CN-H_2O acidified with 0.1% formic acid, 14:86) to yield compounds **12** (29.4 mg) and **13** (49.3 mg). Fraction E2.6 (1.17 g) was separated into five subfractions (E2.6.1-E2.6.5) by silica gel CC with CH_2Cl_2-MeOH (90:1). Subfraction E2.6.2 (202 mg) was purified by preparative HPLC (CH_3CN-H_2O acidified with 0.1% formic acid, 12:88) to give compound **14** (15.8 mg). Subfraction E2.6.1 (445 mg) was subjected to silica gel CC with CH_2Cl_2-EtOAc (60:1) and preparative HPLC (CH_3CN-H_2O, 15:85) to give compound **15** (4.8 mg) and compound **1** (3.0 mg). Compounds **16** (3.0 mg) and **6** (5.1 mg) were obtained from fraction E2.6.3 (122 mg) by preparative HPLC with CH_3CN-H_2O acidified with 0.1% formic acid (11:89) and CH_3CN-H_2O (25:75), respectively. Fraction E2.7 (85 mg) was purified by preparative HPLC (MeOH-H_2O, 35:65) to give compound **11** (13 mg). For fraction E2.8 (161 mg), compounds **3** (1.7 mg) and **2** (8.4 mg) were obtained by silica gel CC eluting with CH_2Cl_2-MeOH (70:1) and preparative HPLC (CH_3CN-H_2O, 21:79). Fraction E5 (8.5 g) was subjected to repeated silica gel CC with CH_2Cl_2-MeOH (60:1–34:1) and an C_{18} reversed-phase silica gel column with MeOH-H_2O (75:25) to yield compound **17** (50 mg). Fraction E7 (5.5 g) was applied to silica gel silica gel CC with CH_2Cl_2-MeOH (24:1) to yield five fractions (E7.1–E7.5). Fraction E7.3 (1.5 g) was purified by an C_{18} reversed-phase silica gel column and preparative HPLC eluted with CH_3CN-H_2O (17:83) to afford compound **5** (1.82 mg). Fraction E1 (7.6 g) was fractioned via silica gel column with PE-EtOAc (50:1–3:1) to give fourteen subfractions (E1.1-E1.14). Fraction E1.2 (658 mg) was purified by silica gel CC with PE-EtOAc (90:1) and Sephadex LH-20 CC (MeOH) to give compound **18** (73 mg). Fraction E1.12 (368 mg) was purified by silica gel CC with CH_2Cl_2-EtOAc (30:1–10:1) and preparative HPLC (MeOH-H_2O, 75:25–80:20) to afford compound **4** (7.1 mg).

2.3.1. 3-Methyl-4-(3-oxobutyl)cyclohepta-2,4,6-trien-1-one (1)

Brown amorphous powder; UV (MeOH) λ_{max} (log ε): 237 (4.20), 318 (1.58) nm; For ^{1}H and ^{13}C NMR spectroscopic data, see Table 1; HRESIMS *m/z* 191.1077 $[M+H]^+$ (calcd for $C_{12}H_{15}O_2$, 191.1072).

2.3.2. Alismaine A (2)

Brown amorphous powder; $[\alpha]_D^{20}$ +33.6 (c 0.06, MeOH); UV (MeOH) λ_{max} (log ε): 270 (4.20) nm; IR ν_{max} 3478, 2937, 1582, 1503, 1460, 1330, 1225, 1120 cm^{-1}; $Mo_2(OAc)_4$-induced ECD (MeOH) 305 ($\Delta\varepsilon$ + 0.31) nm; For ^{1}H and ^{13}C NMR spectroscopic data, see Table 2; HRESIMS *m/z* 449.1818 $[M-H]^-$ (calcd for $C_{23}H_{29}O_9$, 449.1812).

2.3.3. Alismaine B (3)

Brown amorphous powder; $[\alpha]_D^{20}$ +32.0 (c 0.08, MeOH); UV (MeOH) λ_{max} (log ε): 270 (4.11) nm; $Mo_2(OAc)_4$-induced ECD (MeOH) 305 ($\Delta\varepsilon$ + 0.52) nm; For ^{1}H and ^{13}C NMR spectroscopic data, see Table 2; HRESIMS *m/z* 449.1815 $[M-H]^-$ (calcd for $C_{23}H_{29}O_9$, 449.1812).

Table 2
^{1}H (600 MHz) and ^{13}C (150 MHz) NMR data for compounds **2** and **3** in CD_3OD (*J* in Hz).

No.	**2**		**3**	
	δ_H	δ_C	δ_H	δ_C
1		135.1		135.6
2,6		153.2		153.2
3,5	6.71, s	103.5	6.64, s	103.5
4		133.2		133.1
7	6.54, d, 15.8	130.0	6.45, d, 15.8	130.1
8	6.31, dt, 15.8, 5.6	128.4	6.22, dt, 15.8, 5.6	128.2
9	4.23, dd, 5.7, 1.5	62.2	4.12, dd, 5.7, 1.5	62.2
1′		134.8		134.9
2′,6′		147.7		147.8
3′,5′	6.62, s	104.7	6.60, s	104.5
4′		129.3		129.0
7′	4.49, d, 5.8	82.7	4.45, d, 6.4	83.8
8′	4.23, m	85.4	4.15, m	85.1
9′	3.90, dd, 12.1, 4.7; 3.67, dd, 12.1, 3.1	60.0	3.47, dd, 12.0, 4.0; 3.13, dd, 11.9, 4.3	60.6
2,6-OCH_3	3.79, s	55.2	3.74, s	55.2
2′,6′-OCH_3	3.83, s	55.4	3.74, s	55.3
7′-OCH_3	3.29, s	56.0	3.13, s	55.9

2.3.4. 16S, 24S-dihydroxy-24-deacetyl alisol O (4)

White amorphous powder; $[\alpha]_D^{20}$ +32.7 (c 0.05, MeOH); UV (MeOH) λ_{max} (log ε): 250 (4.36) nm; ECD (MeOH) λ_{max} ($\Delta\varepsilon$) 245 (+3.72), 290 (+4.18) nm; IR ν_{max} 3468, 2970, 1700, 1466, 1378, 1018, 829 cm^{-1}; For ^{1}H and ^{13}C NMR spectroscopic data, see Table 3; HRESIMS *m/z* 485.3272 $[M-H]^-$ (calcd for $C_{30}H_{45}O_5$, 485.3267).

2.3.5. Calamusin I (5, racemic mixture)

Brown amorphous powder; UV (MeOH) λ_{max} (log ε): 246 (3.93) nm; (1*S*, 4*S*, 10*R*)-Calamusin I: ECD (MeOH) λ_{max} ($\Delta\varepsilon$) 242 (+2.36), 335 (+0.69) nm; (1*R*, 4*R*, 10*S*)-Calamusin I: ECD (MeOH) λ_{max} ($\Delta\varepsilon$) 242 (−1.73), 331 (−0.99) nm; For ^{1}H and ^{13}C NMR spectroscopic data, see Table 1; HRESIMS *m/z* 211.1341 $[M+H]^+$ (calcd for $C_{12}H_{19}O_3$, 211.1334).

Table 3
^{1}H (600 MHz) and ^{13}C (150 MHz) NMR data for compound **4** (*J* in Hz).

No.	**4** ($CDCl_3$)		**4** (CD_3OD)	
	δ_H	δ_c	δ_H	δ_c
1	2.09, t, 12.4; 1.64, m	33.8	2.13, t, 12.7; 1.67, m	31.9
2	2.71, m; 2.27, m	35.0	2.84, m; 2.20, m	33.1
3		221.4		221.5
4		47.7		46.9
5	2.33, d, 11.6	48.6	2.42, d, 12.3	46.0
6	1.51, m; 1.35, m	20.8	1.55, m; 1.40, m	18.9
7	1.81, dd, 13.1, 6.5; 1.28, m	32.6	1.91, dd, 13.3, 6.8; 1.33, m	30.9
8		39.3		37.7
9	2.22, m	48.3	2.28, m	46.8
10		37.2		35.5
11	5.70, d, 10.3	132.6	5.78, d, 10.3	130.7
12	6.47, dd, 10.3, 3.1	124.3	6.53, dd, 10.3, 2.9	122.6
13		140.1		138.2
14		52.6		51.0
15	2.22, m; 1.70, d, 14.6	40.2	2.19, m; 1.66, m	38.3
16		119.2		117.6
17		135.5		134.5
18	1.00, s	23.8	1.03, s	21.5
19	0.90, s	26.2	0.90, s	23.6
20	2.82, m	29.1	2.81, m	27.5
21	1.29, d, 6.7	21.6	1.28, d, 6.7	19.2
22	1.64, m; 1.64, m	40.2	1.67, m; 1.55, m	38.7
23	4.35, s	75.7	4.40, s	74.0
24	3.76, s	86.3	3.73, s	84.7
25		73.0		70.8
26	1.17, s	26.5	1.10, s	22.6
27	1.19, s	26.9	1.17, s	25.3
28	1.09, s	30.8	1.09, s	28.1
29	1.05, s	20.7	1.04, s	18.3
30	1.07, s	24.6	1.06, s	22.2

2.4. Anti-inflammatory activities in vitro

The NO inhibitory assay was performed according to the reported procedure in the literature [38] with some modifications. Briefly, RAW 264.7 cells were seeded in 96-well plates at a density of 1×10^4 cells per well in a 5% CO_2/95% air incubator for 24 h, then stimulated with 300 ng/mL of LPS in the absence or presence of test compounds (0, 3, 10, 20, 50, and 100 μM), with indomethacin as a positive control (Sigma, St. Louis, MO, USA). After incubation at 37 °C for 24 h, 50 μL of cell-free supernatant was mixed with 100 μL of Griess reagent. The optical density was measured at the wavelength of 546 nm using a microplate reader (Dynex Technologies Inc., Chantilly, USA). The concentration of NO in the medium was measured by assaying the levels of NO^{2-} via the Griess reaction. The IC_{50} values were determined and reported as mean ± SD of three independent experiments.

In order to find whether inhibition of NO production was due to the cytotoxicity of the tested compounds, cell viabilities were also assessed by cell counting kit-8 (CCK-8; Dojindo Molecular Technologies, Tokyo, Japan) according to the manufacturer's instructions.

2.5. Anti-inflammatory activities in zebrafish

2.5.1. Zebrafish maintenance and embryo collection

Zebrafish (*Danio rerio*; wild-type, AB strain) was used in this study. Adult zebrafish were maintained in a semistatic system with charcoal-filtered tap water (pH 7.0–7.4) at 28 °C in a 14-/10-hour day (500 lx)/night light cycle, and fed twice daily with brine shrimp. The embryos were obtained by natural spawning of adult zebrafish (5 months old). Healthy embryos were selected at 24 h post-fertilization (hpf) under a dissecting microscope. Then, the embryos developing normally to the blastula stage were selected for subsequent experiments.

2.5.2. $CuSO_4$-induced inflammation model

$CuSO_4$-induced inflammation model was selected to evaluate anti-inflammatory effects of compounds **4** and **17** according to the previous report [35]. Healthy zebrafish larvae were selected and divided randomly into 6-well plates (n = 15/well) at 72 hpf. Exposure groups were incubated with different concentrations of compound **4** or **17** (3, 10, 20 μM) for 1 h, with indomethacin (50 μM) as a positive control. $CuSO_4$ (20 μM) was supplemented to the exposure groups and model group. The control group was incubated with fresh fish water. Finally, the inflammatory reaction was observed and imaged after the addition of $CuSO_4$ for 1 h. All treatments were performed in triplicate, and all 6-well plates were maintained in a 5 mL final volume of embryo medium. Each zebrafish larva was imaged using a fluorescence microscope (Olympus, SZX16, Tokyo, Japan), and the number of macrophages was recorded using Image-Pro Plus software.

3. Results and discussion

3.1. Structural elucidation

Compound **1** was deduced as $C_{12}H_{14}O_2$ by the HRESIMS (*m/z* 191.1077 $[M+H]^+$ (calcd for $C_{12}H_{15}O_2$, 191.1072), indicating 6 degrees of unsaturation. The ^{1}H NMR spectrum (Table 1) displayed four olefinic protons [δ_H 6.94 (1H, dd, *J* = 11.7, 2.8 Hz), 7.16 (1H, d, *J* = 2.8 Hz), 7.28 (1H, d, *J* = 11.7, 9.1 Hz), and 7.10 (1H, d, *J* = 9.1 Hz)] and two methyl groups [δ_H 2.19 (3H, s), 2.42 (3H, d, *J* = 0.6 Hz)]. The ^{13}C NMR (Table 1) and HSQC spectra showed 12 carbon signals corresponding to two carbonyl carbons (δ_c 207.9, 187.7), six olefinic carbons (δ_c 151.2, 149.9, 141.5, 138.0, 137.5,

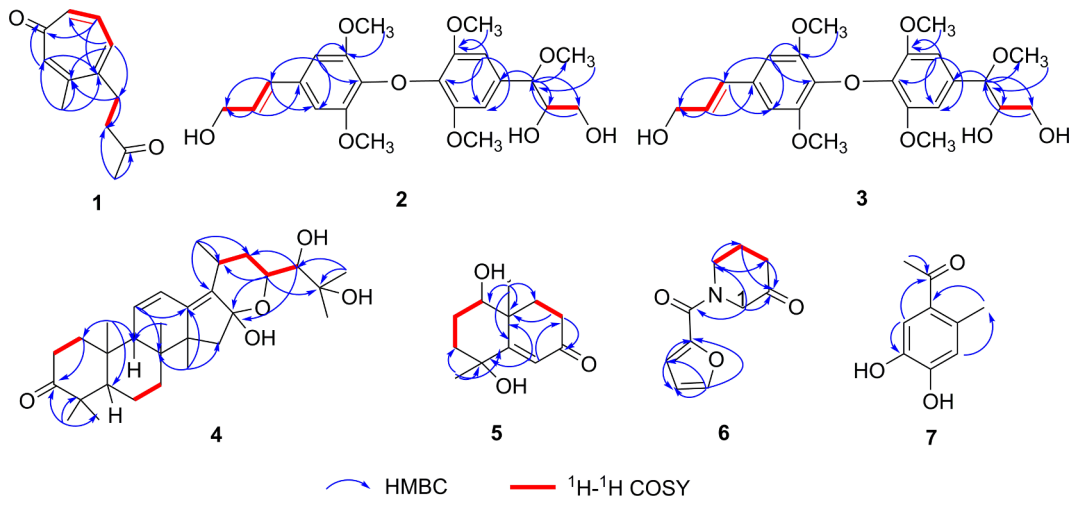

Fig. 2. Selected HMBC, ^{1}H-^{1}HCOSY correlations of compounds **1–7**.

133.3), two methylene carbons (δ_c 42.5, 31.0), and two methyl carbons (δ_c 28.4, 24.4). The ^{1}H-^{1}H COSY correlations (Fig. 2) of H-6 with H-5/H-7 as well as the HMBC correlations (Fig. 2) from H-6 to C-1/C-4, H-5 to C-3/C-7, H-2 to C-1/C-4 indicated the seven-membered ring core. The HMBC correlations (Fig. 2) from H_3-11 to C-9/C-10, H_3-12 to C-2/C-3/C-4 indicated Me-11 and Me-12 were attached to C-10 and C-3, respectively. The structure of side chain was determined and attached to C-4 by the HMBC correlations from H-9 to C-4/C-8/C-10, H-8 to C-9/C-5/C-4 and H-5 to C-8 (Fig. 2). Thus, **1** was elucidated as 3-methyl-4-(3-oxobutyl)cyclohepta-2,4,6-trien-1-one.

Compound **2** had the molecular formula of $C_{23}H_{30}O_9$, as indicated by HRESIMS (*m/z* 449.1818 $[M-H]^-$, calcd for $C_{23}H_{29}O_9$, 449.1812). The ^{1}H NMR spectrum (Table 2) showed signals of two *trans*-olefinic protons [δ_H 6.54 (1H, d, J = 15.8 Hz), 6.31 (1H, dt, J = 15.8, 5.6 Hz)], four aromatic ring protons [δ_H 6.71 (2H, s), 6.62 (2H, s)], six oxygenated protons [δ_H 4.49 (1H, d, J = 5.8 Hz), 4.23 (2H, dd, J = 5.7, 1.5 Hz), 4.23 (1H, m), 3.90 (1H, dd, J = 12.1, 4.7 Hz), 3.67 (1H, dd, J = 12.1, 3.1 Hz)], five methoxyls [δ_H 3.83 × 2 (3H, s), 3.79 × 2 (3H, s), 3.29 (3H, s)]. The ^{13}C NMR, DEPT and HSQC spectra (Table 2) exhibited two *trans*-olefinic carbons (δ_C 130.0, 128.4), twelve aromatic ring carbons (δ_C 153.2 × 2, 147.7 × 2, 135.1, 134.8, 133.2, 129.3, 104.7 × 2, 103.5 × 2), two oxygenated methine carbons (δ_C 85.4, 82.7), two oxygenated methylene carbons (δ_C 62.2, 60.0), and three methyl groups (δ_C 56.0, 55.4, 55.2). The identical ^{1}H and ^{13}C signals of aromatic ring and methoxyl indicated the symmetrical moieties in **2**. The suspect was supported by HMBC correlations (Fig. 2) from H-3 to C-5, H-3′ to C-5′ and 2-OCH_3 to C-2, 2′-OCH_3 to C-2′. A 3-hydroxy-*trans*-prop-1-enyl group attached at C-4 was confirmed by the HMBC correlations from H-7 to C-3/C-5/C-9, H-8 to C-4/C-9 and H-3/5 to C-7. Meanwhile, the HMBC correlations from H-7′ to C-4′/C-8′/C-9′, H-9′ to C-7′, and 7′-OCH_3 to C-7′ indicated 1-methoxy-2,3-dihydroxypropanyl group attached at C-4′ (Fig. 2). The side chain moieties were further confirmed by ^{1}H-^{1}H COSY correlations (Fig. 2). The remaining one oxygen atom should be deposited between the two aromatic rings based on the molecular formula and ^{13}C chemical shifts of C-l and C-l′. The coupling constant (5.8 Hz) observed between H-7′ and H-8′ suggested a *syn*- or *erythro*-configuration of the two protons [39]. The absolute configuration of C-8′ was determined via the $Mo_2(OAc)_4$-induced ECD method developed by Snatzke [2]. The positive Cotton effect at 305 nm indicated a 8′*R* configuration (Fig. 3). Accordingly, the absolute configuration of **2** was determined to be 7′*S*, 8′*R* and named as alismaine A.

The HRESIMS (*m/z* 449.1815 $[M-H]^-$, calcd for $C_{23}H_{29}O_9$, 449.1812), UV, ^{1}H and ^{13}C NMR (Table 3) of compound **3** were quite similar to those of **2**, except for the signals of C-7′ were deshielded from δ_C 82.7 in **2** to δ_C 83.8 in **3** and the chemical shifts of H-9′ shielded from δ_H 3.90, 3.67 in **2** to δ_H 3.47, 3.13 in **3.** The same planar structure was confirmed by HMBC and ^{1}H-^{1}H COSY correlations (Fig. 2). Conformation analysis indicated that the coupling constant of 6.4 Hz (Table 3) between H-7′ and H-8′ was in accord with an *anti*- or *threo*-configuration [39]. The absolute configuration of C-8′ was determined via the $Mo_2(OAc)_4$-induced ECD method. The similar positive Cotton effect to **2** at 305 nm was observed (Fig. 3). Thus, the absolute configuration of **3** was determined to be 7′*R*, 8′*R* and named as alismaine B.

Compound **4** was assigned a molecular formula of $C_{30}H_{46}O_5$ by the HRESIMS (*m/z* 485.3272 $[M-H]^-$, calcd for $C_{30}H_{45}O_5$, 485.3267). The ^{1}H NMR (Table 3) showed two olefinic protons [δ_H 6.47 (1H, dd, J = 10.3, 3.1 Hz), 5.70 (1H, d, J = 10.3 Hz)], two oxygenated protons [δ_H 4.35 (1H, s), 3.76 (1H, s)], and eight methyl groups [δ_H 0.90, 1.00, 1.05, 1.07, 1.09, 1.17, 1.19 (each 3H, s), and 1.29 (3H, d, J = 6.7 Hz)]. The ^{13}C NMR (Table 3) and HSQC data revealed 30 carbon resonances, including one carbonyl (δ_c 221.4), four olefinic carbons (δ_c 140.1, 135.5, 132.6, 124.3), four oxygenated carbons (δ_c 119.2, 86.3, 75.7, 73.0), eight methyls (δ_c 30.8, 26.9, 26.5, 26.2, 24.6, 23.8, 21.6, 20.7). The NMR spectral analysis revealed that **4** should be a protostane-type triterpenoid. The ^{1}H and ^{13}C NMR data were very similar to those of 24-deacetyl alisol O, which had been isolated from *A. orientale* [40], except for the oxygenated quaternary carbon (δ_c 119.2) in **4** instead of an oxygenated methine [δ_H 4.58 (1H, br d, J = 8.0 Hz); δ_c 80.5] in 24-deacetyl alisol O at C-16. The deduction was also confirmed by the HMBC correlations (Fig. 2) from H-15/H-23/H-24 to C-16. The present of a hydroxyl could also account for the one more oxygen atom in **4**, compared with 24-deacetyl alisol O. In addition, the downfield shifts of C-24 from δ_c 76.3 in 24-deacetyl alisol O to δ_c 86.3 in **4** indicated the different configuration. The relative configuration was established by analysis of NOESY data. Correlations of H-5 with H_3-18, of H-9 with H_3-30/H_3-19, of H_3-30 with H-24, of H-24 with H-20 and H-22b (β), of H-22a (α) with H-23 (Fig. 3) demonstrated that H_3-30, H-9, H_3-19, H-24 and H-20 were β-oriented, whereas H-5, H_3-18, OH-24, H-23, H_3-21 and OH-16 occupied the opposite face. The positive Cotton effect (245 nm, +3.73) observed in the CD spectrum (Fig. 4) indicated a 14 *R* configuration, which was consistent with the absolute configurations at C-14 of the protostane skeleton [41]. Accordingly, the structure of **4** was elucidated, compared with compound 24-deacetyl alisol O, and named as 16*S*, 24*S*-dihydroxy-24-deacetyl alisol O.

Compound **5** was deduced to have a molecular formula of $C_{12}H_{18}O_3$ by HRESIMS (*m/z* 211.1341 $[M+H]^+$, calcd for $C_{12}H_{19}O_3$, 211.1334). The ^{1}H NMR spectrum (Table 1) displayed signals corresponding to two methyl groups [δ_H 1.23 (3H, s), 1.31 (3H, s)], an olefinic proton [δ_H 6.26 (1H, s)] and an oxygenated methine proton [δ_H 3.43 (1H, m)]. The ^{13}C NMR (Table 1) and HSQC spectra exhibited 12 signals, including

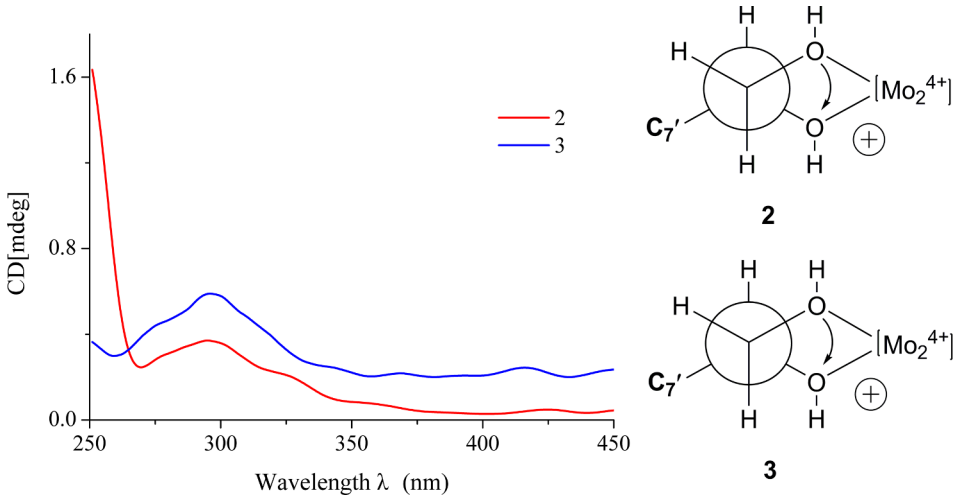

Fig. 3. $Mo_2(OAc)_4$-induced ECD spectra and preferred conformation of the 8′,9′-diol moiety in the chiral Mo complex of compounds **2** and **3**.

one carbonyl carbon (δc 201.7), two olefinic carbons (δc 176.5, 123.8), four methylenes (δc 33.6, 33.4, 33.2, 26.0), one methine (δc 73.0), two quaternary carbons (δc 71.0, 40.9), and two methyls (δc 29.4, 22.9). The ^1H and ^{13}C NMR data closely resembled those of calamusin I, a norsesquiterpene isolated from the rhizome of *Acorus calamus* [42]. However, a distinctive difference in the ^{13}C NMR spectrum was observed between these two molecules. The chemical shifts of C-1/C-3/C-9 (δ_c 78.3, 39.3, 38.5) in calamusin I were downfield in comparison with those of **5** (δ_c 73.0, 33.6, 33.4). The HMBC correlations (Fig. 2) from H_3-12 to C-3/C-4/C-5, H_3-11 to C-1/C-5/C-9/C-10, H-6 to C-4/C-8/C-10, H-8 to C-7/C-10 and ^1H-^1H COSY correlations (Fig. 2) between H-1 and H-2, H-2 and H-3, H-8 and H-9 suggested that **5** possessed the same planar structure as calamusin I. The relative configuration of **5** was established on the basis of NOESY correlations (Fig. 5) between H_3-12 and H-3a (*α*), H-3b (*β*) and H-1, H-1 and H_3-11, indicating that H-1, Me-11 were *β*-oriented and Me-12 was *α*-oriented. However, Me-11 is *α*-oriented in calamusin I. ECD method was used to determine the absolute configuration of **5**, but the ECD spectrum did not show any Cotton effects, indicating that **5** comprised a racemic mixture. Chiral HPLC analysis and the CD spectra (Fig. 6) of the resolved enantiomers (**5a** and **5b**) confirmed that **5** was a racemic mixture. The absolute configuration of compounds **5a** and **5b** was determined by comparing experimental and calculated ECD spectra (Fig. 6). The theoretical calculation of ECD was performed using time dependent Density Functional Theory (TDDFT) at B3LYP/6-31G (d,p) level in MeOH with PCM model. The

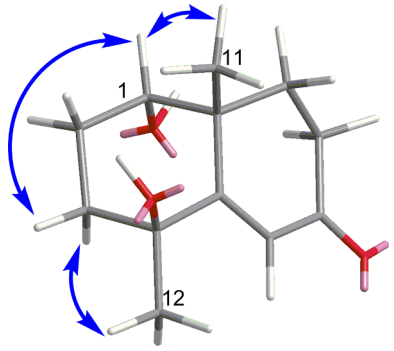

Fig. 5. Selected NOESY correlations of compound **5**.

experimental ECD spectra of **5a** and **5b** was consistent with the calculated ECD spectra of (1*S*, 4*S*, 10*R*)-**5** and (1*R*, 4*R*, 10*S*)-**5**, respectively. Thus, compound **5a** was determined to be (1*S*, 4*S*, 10*R*)-Calamusin I and compound **5b** was determined to be (1*R*, 4*R*, 10*S*)-Calamusin I.

Compounds **6** and **7** were determined as 1-(furan-2-carbonyl)piperidin-3-one and 1-(4,5-dihydroxy-2-methylphenyl)-Ethanone, respectively, by their ^1H and ^{13}C NMR spectra (Table 1) as well as HMBC and ^1H-^1H COSY correlations (Fig. 2). Compound **6** was a commercial product, searched in SciFinder, and compound **7** was previously reported as a synthetic product [43]. They were both reported as natural

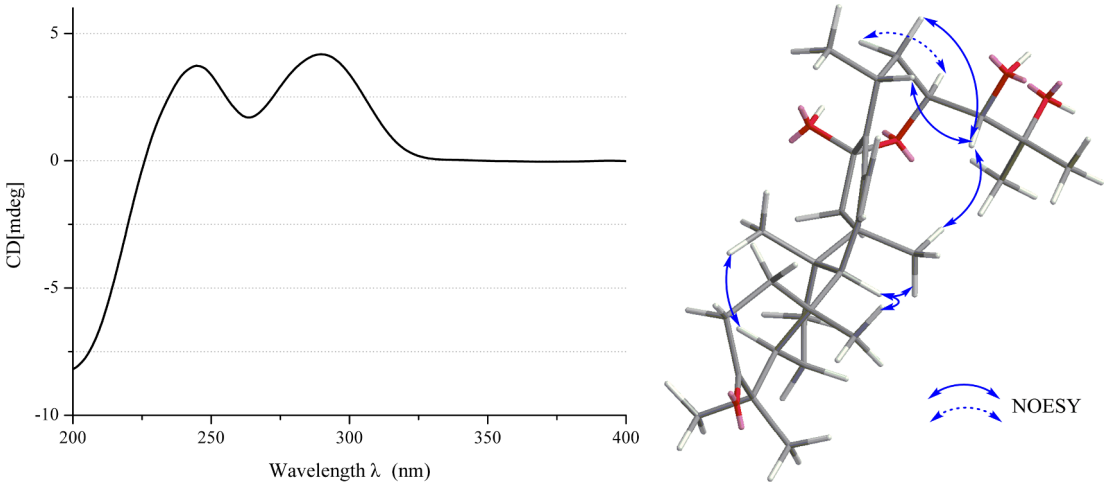

Fig. 4. Experimental ECD spectra and selected NOESY correlations of compound **4**.

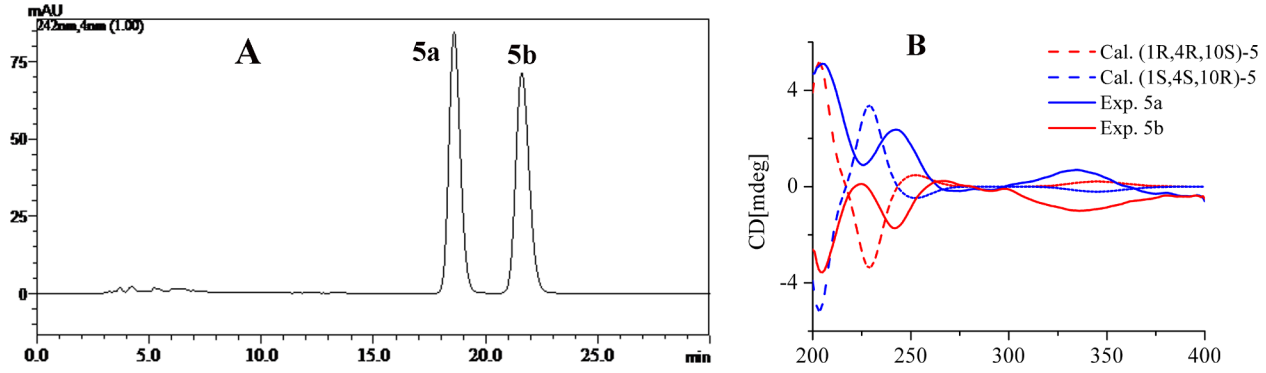

Fig. 6. HPLC profiles of compound **5** [A, column, Daicel Chiralpak® IE (5 μm, 4.6 × 250 mm); mobile phase, *n*-hexane/2-propanol = 7:3; flow rate: 1 mL/min; UV detection at 242 nm; peak area of **5a**:**5b** = 1:1] and calculated and experimental ECD spectra of compound **5a** and **5b** in MeOH (B).

products for the first time.

On the basis of the literature and spectroscopic data, the other eleven known ones were defined as p-hydroxybenzoic acid (**8**) [44], vanillic acid (**9**) [45], protocatechualdehyde (**10**) [46], syringaresinol (**11**) [47], 6-methoxychroman-2-one (**12**) [48], ferulic acid (**13**) [49], syringic acid (**14**) [50], cyclo-(L-Pro-D-Leu) (**15**) [51], syringaldehyde (**16**) [52], 16-oxo-11-anhydroalisol A (**17**) [2], dibutyl phthalate (**18**) [53], of which compounds **8–10**, **12**, **14–16**, and **18** were reported from AR for the first time.

3.2. Inhibitory effects on NO production in vitro

In this study, the anti-inflammatory effects of compounds **2**, **4**, **8**, **9**, **12–15**, and **17** were evaluated by measuring the inhibitory effect on LPS-induced NO production in RAW 264.7 macrophage cells. As shown in Table 4 and Fig. 7, the two protostane-type triterpenoids, compounds **4** (IC_{50} = 39.26 ± 2.75 μM) and **17** (IC_{50} = 63.87 ± 1.95 μM) exhibited potent inhibitory effects on NO production compared with indomethacin (IC_{50} = 34.87 ± 2.19 μM). Their inhibitory effects were in dose-dependent manner. However, the other compounds showed very weak inhibitory effects with IC_{50} values greater than 100 μM. Cytotoxic activities of compounds **4** and **17** against RAW 264.7 macrophages were tested by CCK-8 assay, with the relative cell viabilities as an index. As shown in Fig. 7, compound **17** exhibited no significant cytotoxicity at the effective concentration for the inhibition on NO production. However, the relative cell viability of compound **4** at the concentration of 100 μM declined by half compared with that at the concentration of 50 μM, indicating the possible cytotoxicity of it. Thus, the NO inhibition of compound **4** at the concentration of 100 μM was inauthentic and the IC_{50} value of it for the inhibition on NO production was caculated based on the data from the concentrations of 3 to 50 μM.

Table 4
Inhibitory effects of the compounds isolated from AR on NO production induced by LPS in RAW 264.7.

Compounds	NO inhibition ratio (%)	IC_{50} (mean ± SD, μM)	
		NO inhibitory assay	CCK-8 assay
2	38.88 ± 1.05b	> 100	–
4	61.28 ± 3.24 a	39.26 ± 2.75	> 50
8	19.79 ± 2.14b	> 100	–
9	27.91 ± 1.09b	> 100	–
12	24.95 ± 0.80b	> 100	–
13	24.06 ± 0.92b	> 100	–
14	41.59 ± 1.42b	> 100	–
15	25.67 ± 0.43b	> 100	–
17	63.14 ± 2.35b	63.87 ± 1.95	> 100
Indomethacin[c]	56.61 ± 2.05 a	34.87 ± 2.19	–

a: tested in 50 μM, b: tested in 100 μM; c: positive control; – not detected.

3.3. Anti-inflammatory effects of compounds 4 and 17 in zebrafish

$CuSO_4$ could induce acute inflammation in zebrafish, as characterized by the rapid migration of macrophages to the nerve eminence. The anti-inflammatory drugs cause these macrophages to return and the quantity of macrophages in the region of the neuromast were used to evaluate the anti-inflammatory activities [35]. As shown in Fig. 8B and C, large numbers of macrophages migrated to the neuromast after induced by $CuSO_4$ indicating the inflammation model was established successfully. Compounds **4** and **17** could significantly inhibit $CuSO_4$-induced migration of macrophages toward the neuromast at the concentrations of 10 and 20 μM, compared with the $CuSO_4$ group. Their effects were comparable with the positive control. Thus, the potent anti-inflammatory effects of compounds **4** and **17** were further confirmed in zebrafish model.

Meanwhile, the inhibitory activities on NO production of the protostane triterpenoids, such as 16-oxo-11-anhydroalisol A 24-acetate, alisol F, 25-anhydroalisol F, and alisol B 23-acetate were also reported [2], of which alisol B 23-acetate exerted inhibitory effects by suppression of iNOS mRNA expression [54]. In addition, anti-inflammatory effects and related mechanisms of protostane triterpenoids were also revealed in different ways, of which alisol B and alisol B 23-acetate significantly inhibited leukotriene and β-hexosaminidase release between 1 and 10 μM and delayed-type hypersensitivity response [23]; alisol A 24-acetate could inhibit inflammatory cytokines TNF-alpha, IL-6 levels in non-alcoholic fatty liver disease [15]. On the basis of the present results and literature analyses mentioned above, protostane-type triterpenoids may be responsible for the anti-inflammatory activities of AR and the anti-inflammatory mechanisms of compounds **4** and **17** need to be further studied.

4. Conclusions

In conclusion, the investigation on the aqueous extract of AR led to the isolation and structure elucidation of nineteen compounds, including six new ones, two new natural products, as well as eleven known ones, of which eight were reported from AR for the first time. These compounds involved multiple chemical types, such as 2, 4, 6-cycloheptatrien ketone, diphenylpropanoid ethers, protostane-type triterpenoid, norsesquierpene, phenolic acid, coumarin, and cyclic peptide, which indicated the structural diversities of the compounds in the aqueous extract of AR. Just as the discussion in the introduction, with regard to the unknown compounds in the aqueous extract of AR, there was still an enormous amount of work to be done. The isolated protostane-type triterpenoids, compounds **4** and **17**, exerted potent NO inhibitory activities in RAW 264.7 cells. Their anti-inflammatory effects were also confirmed in zebrafish model. Based on the available results, protostane-type triterpenoids might be the main active ingredients for the anti-inflammatory activities of AR. The investigation would be

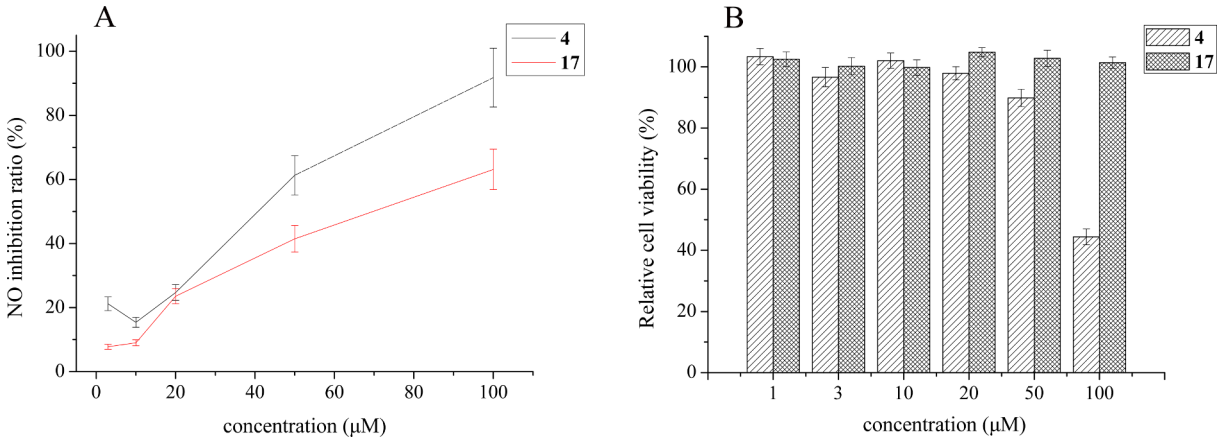

Fig. 7. NO inhibition ratio (A) and relative cell viability (B, compared with the control) of compounds **4** and **17** at different concentrations in RAW 264.7 macrophages. Data are expressed as the mean ± SD (n = 3).

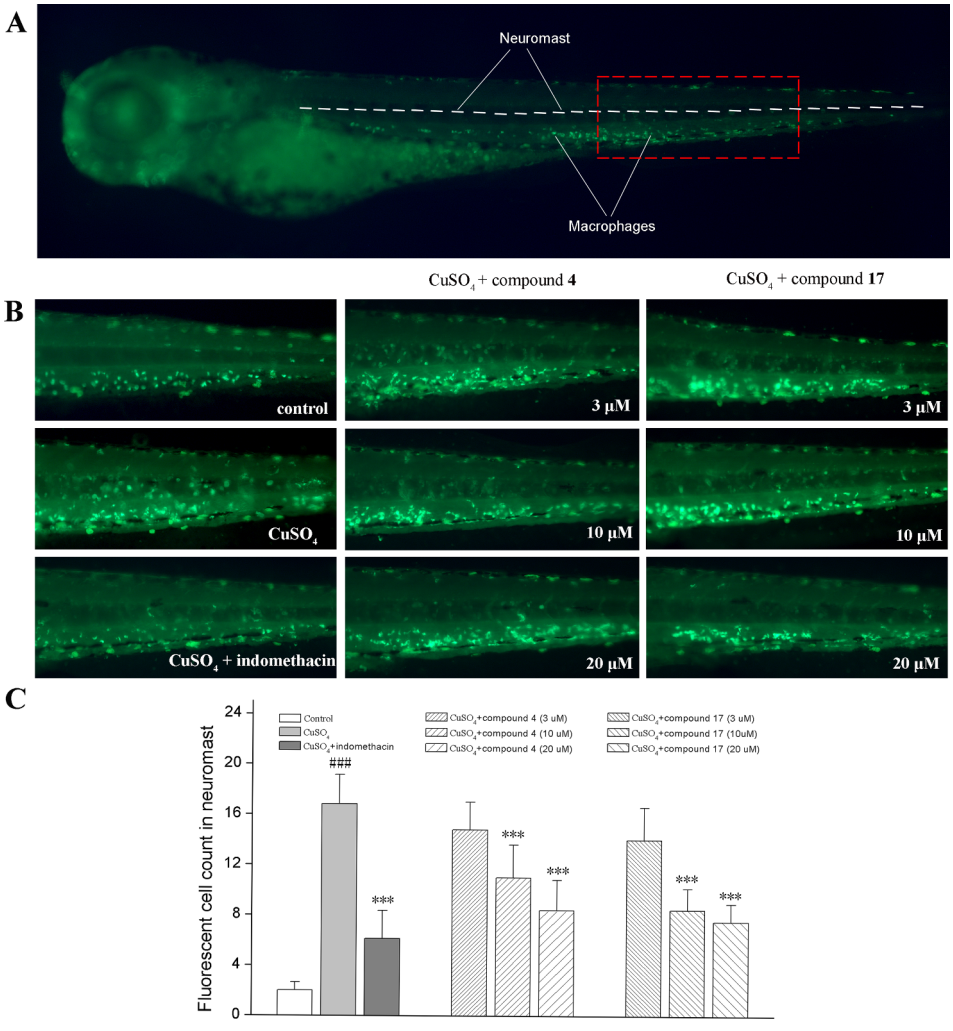

Fig. 8. Compounds **4** and **17** alleviated the inflammation response in zebrafish after $CuSO_4$ exposure. (A) Diagram of a normal zebrafish (the field of view was in red rectangle); (B) Representative images of zebrafish treated with compounds **4, 17** and $CuSO_4$; (C) Macrophages in the region of the neuromast were quantitatively analyzed. The data are represented as the mean ± SD. ###p < 0.001 vs. the control group, ***p < 0.001 vs. the $CuSO_4$ group.

helpful to reveal the bioactive constituents and provided important evidences for the development of AR.

Declaration of Competing Interest

The authors declare no competing financial interest.

Acknowledgements

This research was supported by the National Traditional Chinese Medicine Standardization Project (No. ZYBZH-C-JL-24), research subject on the revision of pharmaceutical standards of Chinese Pharmacopoeia Commission (No. 2018Z079), National Science Foundation for Young Scientists of China (No. 81802629), the Youth Fund of Shandong Academy of Sciences (No. 2018QN0024), the Industry-University-Research Collaborative Innovation Major Projects in Guangzhou Science and Technology Programs 2016 (No. 201604046012, No. 201604046013).

Appendix A. Supplementary material

Supplementary data to this article can be found online at https://doi.org/10.1016/j.bioorg.2019.103226.

References

[1] Z.Y. Wu, P.H. Raven, Flora of China, Missouri Botanical Garden Press and Science Press, St. Louis and Beijing, 2008.
[2] Z.P. Mai, K. Zhou, G.B. Ge, C. Wang, X.K. Huo, P.P. Dong, S. Deng, B.J. Zhang, H.L. Zhang, S.S. Huang, X.C. Ma, J. Nat. Prod. 78 (2015) 2372–2380.
[3] J.Y. Chen, H.L. Su, Y.J. Huang, P.S. Ge, Z.Q. Lv, J. Chin. Mat. Med. 34 (2009) 2713–2717.
[4] L.L. Zhang, W. Xu, Y.L. Xu, X. Chen, M. Huang, J.J. Lu, Ann. N. Y. Acad. Sci. 1401 (2017) 90–101.
[5] Z. Zhang, D. Wang, Y. Zhao, H. Gao, Y.H. Hu, J.F. Hu, Nat. Prod. Res. 23 (2009) 1013–1020.
[6] Z.Y. Zhao, Q. Zhang, Y.F. Li, L.L. Dong, S.L. Liu, Carbohydr. Polym. 119 (2015) 101–109.
[7] X.L. Xin, Z.L. Yu, X.G. Tian, J.C. Wei, C. Wang, X.K. Huo, J. Ning, L. Feng, C.P. Sun, S. Deng, B.J. Zhang, H.L. Zhang, X.Y. Zhao, G.J. Fan, Phytochem. Lett. 21 (2017) 46–50.
[8] Z. Shu, J. Pu, L. Chen, Y. Zhang, K. Rahman, L. Qin, C. Zheng, Am. J. Chin. Med. 44 (2016) 227–251.
[9] Y.L. Feng, H. Chen, T. Tian, D.Q. Chen, Y.Y. Zhao, R.C. Lin, J. Ethnopharmacol. 154 (2014) 386–390.
[10] D.Q. Chen, Y.L. Feng, T. Tian, H. Chen, L. Yin, Y.Y. Zhao, R.C. Lin, J. Ethnopharmacol. 157 (2014) 114–118.
[11] X. Zhang, X.Y. Li, N. Lin, W.L. Zhao, X.Q. Huang, Y. Chen, M.Q. Huang, W. Xu, S.S. Wu, Molecules (Basel, Switzerland) 22 (2017) 1459.
[12] M.K. Jang, Y.R. Han, J.S. Nam, C.W. Han, B.J. Kim, H.S. Jeong, K.T. Ha, M.H. Jung, Int. J. Mol. Sci. 16 (2015) 26151–26165.
[13] Y.J. Park, M.S. Kim, H.R. Kim, J.M. Kim, J.K. Hwang, S.H. Yang, H.J. Kim, D.S. Lee, H. Oh, Y.C. Kim, D.G. Ryu, Y.R. Lee, K.B. Kwon, Evidence-Based Complementary Altern. Med. (2014), https://doi.org/10.1155/2014/415097.
[14] F. Xu, H. Yu, C. Lu, J. Chen, W. Gu, Evidence-Based Complementary Altern. Med. (2016), https://doi.org/10.1155/2016/4753852.
[15] L. Zeng, W.J. Tang, J.J. Yin, L.J. Feng, Y.B. Li, X.R. Yao, B.J. Zhou, Cell. Physiol. Biochem. 40 (2016) 453–464.
[16] C.H. Lau, C.M. Chan, Y.W. Chan, K.M. Lau, T.W. Lau, F.C. Lam, C.T. Che, P.C. Leung, K.P. Fung, Y.Y. Ho, C.B. Lau, Phytother. Res. 22 (2008) 1384–1388.
[17] X.H. Xue, X.M. Zhou, W. Wei, T. Chen, Q.P. Su, J. Tao, L.D. Chen, J. Vasc. Res. 53 (2016) 291–300.
[18] A.F. Zhang, Y.Q. Sheng, M.C. Zou, Biomed. Pharmacother. 87 (2017) 110–117.
[19] C.C. Chou, S.L. Pan, C.M. Teng, J.H. Guh, Eur. J. Biomed. 19 (2003) 403–412.
[20] J.X. Wang, H.Z. Li, X.N. Wang, T. Shen, S.Q. Wang, D.M. Ren, Biochem. Biophys. Res. Commun. (2018), https://doi.org/10.1016/j.bbrc.2018.10.022.
[21] L.L. Zhang, Y.L. Xu, Z.H. Tang, X.H. Xu, X. Chen, T. Li, C.Y. Ding, M.Q. Huang, X.P. Chen, Y.T. Wang, X.F. Yuan, J.J. Lu, Phytomedicine 23 (2016) 800–809.
[22] M. Kubo, H. Matsuda, N. Tomohiro, M. Yoshikawa, Biol. Pharm. Bull. 20 (1997) 511–516.
[23] J.H. Lee, O.S. Kwon, H.G. Jin, E.R. Woo, Y.S. Kim, H.P. Kim, Biol. Pharm. Bull. 35 (2012) 1581–1587.
[24] H. Matsuda, T. Kageura, I. Toguchida, T. Murakami, A. Kishi, M. Yoshikawa, Bioorg. Med. Chem. Lett. 9 (1999) 3081–3086.
[25] C.W. Han, M.J. Kwun, K.H. Kim, J.Y. Choi, S.R. Oh, K.S. Ahn, J.H. Lee, M. Joo, J. Ethnopharmacol. 146 (2013) 402–410.
[26] S.M. Lee, J.H. Kim, Y. Zhang, R.B. An, B.S. Min, H. Joung, H.K. Lee, Arch. Pharmacal Res. 26 (2003) 463–465.
[27] C.W. Han, E.S. Kang, S.A. Ham, H.J. Woo, J.H. Lee, H.G. Seo, Pharm. Biol. 50 (2012) 1281–1288.
[28] M. Tomoda, R. Gonda, N. Shimizu, N. Ohara, Biol. Pharm. Bull. 17 (1994) 572–576.
[29] M. Tomoda, R. Gonda, N. Shimizu, N. Ohara, Pharmacol. Lett. 3 (1993) 147.
[30] N. Shimizu, S. Ohtsu, M. Tomoda, R. Gonda, N. Ohara, Biol. Pharm. Bull. 17 (1994) 1666–1668.
[31] X.Y. Zhao, G. Wang, Y. Wang, X.G. Tian, J.C. Zhao, X.K. Huo, C.P. Sun, L. Feng, J. Ning, C. Wang, B.J. Zhang, X. Wang, Nat. Prod. Res. (2017), https://doi.org/10.1080/14786419.2017.1380024.
[32] C.J. Neumann, Semin. Cell Dev. Biol. 13 (2002) 469.
[33] F.B. Pichler, S. Laurenson, L.C. Williams, A. Dodd, B.R. Copp, D.R. Love, Nat. Biotechnol. 21 (2003) 879–883.
[34] N. Iwanami, Exp. Hematol. 42 (2014) 697–706.
[35] J.J. Li, Y. Zhang, L.W. Han, Q.P. Tian, Q.X. He, X.M. Wang, C. Sun, J. Han, K.C. Liu, Fish Shellfish Immunol. 83 (2018) 205–212.
[36] Y.H. Gui, W.H. Jiao, M. Zhou, Y. Zhang, D.Q. Zeng, H.R. Zhu, K.C. Liu, F. Sun, H.F. Chen, H.W. Lin, Org. Lett. (2019), https://doi.org/10.1021/acs.orglett.8b04019.
[37] E.Y. Ko, S.J. Heo, S.H. Cho, W. Lee, S.Y. Kim, H.W. Yang, G. Ahn, S.H. Cha, S.H. Kwon, M.S. Jeong, K.P. Lee, Y.J. Jeon, K.N. Kim, Int. Immunopharmacol. 67 (2019) 98–105.
[38] F.Z. Yao, Y.Y. Huang, Y.H. Wang, X.J. He, Ind. Crops Prod. 125 (2018) 454–461.
[39] S.G. Liao, Y. Wu, J.M. Yue, Helv. Chim. Acta 89 (2006) 73–80.
[40] A.C. Zhou, C.F. Zhang, M. Zhang, Chin. J. Nat. Med. 6 (2008) 109–111.
[41] M. Zhao, T. Godecke, J. Gunn, J.A. Duan, C.T. Che, Molecules (Basel, Switzerland) 18 (2013) 4054–4080.
[42] Z.Y. Hao, D. Liang, H. Luo, Y.F. Liu, G. Ni, Q.J. Zhang, L. Li, Y.K. Si, H. Sun, R.Y. Chen, D.Q. Yu, J. Nat. Prod. 75 (2012) 1083–1089.
[43] K. Chiba, M. Jinno, R. Kuramoto, M. Tada, Tetrahedron Lett. 39 (1998) 5527–5530.
[44] H.P. Wang, F. Cao, X.W. Yang, Chin. Tradit. Herb. 44 (2013) 24–30.
[45] M.M. Feng, Y.X. Zhang, B. Xia, D.H. He, L.S. Ding, Y. Zhou, X.X. Ye, Chin. Tradit. Herb. Drugs 44 (2013) 2650–2656.
[46] Z.Q. Fu, H.Z. Huang, J. Lin, W.D. He, M.M. Ji, W. Xu, S.M. Fan, Chin. Tradit. Herb. Drugs 46 (2015) 1583–1588.
[47] K. Zhao, Y. Jiang, P.F. Xue, P.F. Tu, Chin. Tradit. Herb. Drugs 44 (2013) 2358–2363.
[48] C. Ding, W. Zhang, J. Li, J. Lei, J. Yu, Nat. Prod. Res. 27 (2013) 1691–1694.
[49] L.J. Meng, B.L. Liu, Y. Zhang, G.X. Zhou, Chin. Tradit. Herb. Drugs 45 (2014) 2139–2142.
[50] L. Shao, W.H. Huang, C.F. Zhang, L. Wang, M. Zhang, Z.T. Wang, China J. Chin. Mater. Med. 33 (2008) 1693–1695.
[51] Y. Li, F. Wang, P.Z. Zhang, M. Yang, China J. Chin. Mater. Med. 38 (2015) 2038–2041.
[52] Y.P. Zhang, S.F. Han, H. Fang, Q.L. Xie, Chin. J. Mar. Drugs 35 (2016) 55–59.
[53] Y.W. Wang, Z.F. Li, M.Z. He, Y.L. Feng, Q. Wang, X. Li, S.L. Yang, Chin. Tradit. Herb. Drugs 44 (2013) 2974–2976.
[54] N.Y. Kim, T.H. Kang, H.O. Pae, B.M. Choi, H.T. Chung, S.W. Myung, Y.S. Song, D.H. Sohn, Y.C. Kim, Pharm. Bull. 22 (1999) 1147–1149.